6-1-2011

Deuterium ion-surface interactions of liquid-lithium thin films on micro-porous molybdenum substrates

Bryan Heim
Birck Nanotechnology Center, Purdue University, bheim@purdue.edu

C. N. Taylor
Purdue University

D. M. Zigon
Purdue University

S. O'Dell
Plasma Proc Inc

Jean Paul Allain
Birck Nanotechnology Center, Purdue University, allain@purdue.edu

Nuclear Instruments and Methods in Physics Research B 269 (2011) 1262–1265

Contents lists available at ScienceDirect

Nuclear Instruments and Methods in Physics Research B

journal homepage: www.elsevier.com/locate/nimb

Deuterium ion–surface interactions of liquid-lithium thin films on micro-porous molybdenum substrates

B. Heim [a,b,*,1], C.N. Taylor [a], D.M. Zigon [a], S. O'Dell [c], J.P. Allain [a,b]

[a] Purdue University, West Lafayette, 400 Central Drive, IN 47907, USA
[b] Birck Nanotechnology Center, Purdue University, West Lafayette, IN 47907, USA
[c] Plasma Processes, Inc., 4914 Moores Mill Road, Huntsville, AL 35811, USA

ARTICLE INFO

Article history:
Received 20 October 2010
Received in revised form 3 January 2011
Available online 7 January 2011

Keywords:
Lithium
Ion–surface analysis
Molybdenum
Ion–surface interactions
Liquid lithium diverter
Percolation

ABSTRACT

Lithium has been utilized to enhance the plasma performance for a variety of fusion devices such as TFTR, CDX-U and NSTX. Lithium in both the solid and liquid states has been studied extensively for its role in hydrogen retention and reduction in sputtering yield. A liquid lithium diverter (LLD) was recently installed in the National Spherical Torus Experiment (NSTX) fusion reactor to investigate lithium applications for plasma-facing surfaces (PFS). Representative samples of LLD material were exposed to lithium depositing and simulated plasma conditions offline at Purdue University to study changes in surface chemical functionalities of Mo, O, Li and D. X-ray photoelectron spectroscopy (XPS) conducted on samples revealed two distinct peak functionalities of lithiated porous molybdenum exposed to deuterium irradiation. The two-peak chemical functionality noticed in porous molybdenum deviates from similar studies conducted on lithiated graphite; such deviation in data is correlated to the complex surface morphology of the porous surface and the correct "wetting" of lithium on the sample surface. The proper lithium "wetting" on the sample surface is essential for maximum deuterium retention and corresponding LLD pumping of deuterium.

1. Introduction

Lithium has been exploited to enhance the plasma performance for a variety of fusion devices such as TFTR, CDX-U and NSTX. Solid lithium was recently studied for its ability to retain hydrogen [1,2]. Improvements in plasma performance through lithium wall conditioning include edge localized mode (ELM) reduction, increased electron temperature, and decreased plasma density [3,4]. In addition to the studies of solid lithium as a plasma-facing surface, the intrinsic properties of liquid lithium compared to solid lithium yielded higher hydrogen/deuterium retention and sputtering yield at temperatures about 50% higher than the lithium melting point [5–8]. These observations spurred interest in liquid plasma facing components (PFC) in tokamak reactors utilizing liquid lithium including CDX-U [9], FTU, and T-11M [10].

With the success of CDX-U [9] and experimental data demonstrating attractive deuterium retention properties of liquid lithium, NSTX recently implemented a liquid lithium diverter (LLD) to study lithium's role in plasma performance, primarily hydrogen pumping and as a self-healing lithium PFC [11]. Two lithium evaporators (LITERS) in NSTX currently supply the diverter region with 10–70 mg/min of lithium coverage [3] that fill the LLD with desired lithium quantities. Resistive heating drives the LLD temperature to ~220 °C to melt the lithium. The LLD is constructed from porous molybdenum (0.152 mm) on a stainless steel platform. A porous molybdenum substrate was chosen to be the material makeup of the LLD, because it emulates properties of lithium loading of the capillary porous systems within lithium limiters in T-11M and FTU [11]. Several studies have investigated lithium loading of porous molybdenum structure [12]; however; the effect of a porous structure on the lithium surface chemistry and the effects of the ion–solid interactions remain unknown.

In order to understand the surface chemistry of evaporated lithium on a porous molybdenum structure and following deuterium ion–surface interactions, surface science facilities at Purdue University Birck Nanotechnology Center and the Particle and Radiation Interaction with Hard and Soft Matter experimental facility (PRISHM) utilized excitation and characterization sources to replicate the PFC environment, and compared the results to well documented surface chemistry of lithiated graphite [2,13].

2. Experimental setup

The porous molybdenum samples were produced by Plasma Processes, Inc. using Vacuum Plasma Spray (VPS) forming techniques.

* Corresponding author at: 400 Central Drive, West Lafayette, IN 47907, USA. Tel.: +1 765 494 5739.
E-mail address: bheim@purdue.edu (B. Heim).
[1] Presenting author.

0168-583X/$ - see front matter © 2011 Elsevier B.V. All rights reserved.
doi:10.1016/j.nimb.2011.01.001

VPS processing was implemented to prevent oxidation of the deposits and substrates during fabrication of the porous molybdenum samples. The required porosity in the molybdenum deposits was produced with off-normal spray parameters. Prior to loading in the VPS chamber, the surface of the stainless steel substrates were grit blasted with alumina grit to remove surface contamination and produce an anchor pattern for the porous molybdenum coating. The substrates were then loaded in the VPS chamber, which was then evacuated and backfilled with high purity argon to the desired spray pressure. During deposition of the porous molybdenum samples, gun motion and part manipulation were computer numerically controlled (CNC) in a rectilinear pattern to ensure repeatability. The thickness was achieved by controlling the number of spray passes and the amount of powder fed to the plasma gun. After molybdenum deposition, the plasma gun was turned off and the parts were allowed to cool to room temperature in the vacuum chamber under a partial pressure of argon.

Samples were loaded into an ultra-high vacuum (UHV) Omicron surface characterization suite located at Birck Nanotechnology Center at Purdue University. The Omicron cluster is broken into two connecting chambers linking a variety of modification and characterization techniques. The sample was loaded into a load lock chamber and transferred to the prep chamber with a base pressure of 2×10^{-9} Torr. The prep chamber houses an Omicron ISE-10 ion gun and a custom-made lithium evaporation and deposition system (LEDS) that evaporates lithium at a rate of 0.1–4 nm/s onto a substrate. The lithium deposition was monitored using a quartz crystal microbalance (QCM) and further verified using X-SEM. A 6.5% error was observed in the deposition thickness on samples after cross calibrating the QCM and X-SEM. Before and after lithium deposition and deuterium irradiation, in-vacu X-ray photoelectron spectroscopy (XPS) characterization was performed with the chamber held at 4×10^{-10} Torr. XPS measurements were performed using a non-monochromatic Al Kα X-ray source at 1486.6 eV, and emitted photoelectrons were collected using a hemispherical energy analyzer (Omicron EA 125 Energy Analyzer).

The Omicron system simulated lithium deposition and single-effect plasma material interactions in NSTX (e.g. mono-energetic ion beam, fixed angle of incidence, and steady surface temperature). Samples were exposed to a pre-determined thickness of lithium coordinated directly to the LITER lithium deposition on the LLD surface [7]. During LITER evaporation and plasma operations, the NSTX LLD surface was heated to ~220 °C to melt lithium coatings. To replicate this phase change, samples were heated to ~220 to 250 °C during both lithium deposition and deuterium irradiation. Experimental layout followed conditions in NSTX, which called for a 40% fill of the LLD surface with lithium. LITER lithium thickness on LLD was converted to 3 μm on 1-cm diameter porous molybdenum samples. After evaporating lithium on LLD samples, post lithiated samples were exposed to 1 kev deuterium ions (500 eV/amu) flux $\sim 10^{13}$ cm^{-2} s^{-1} for a variety of fluences then transferred in-vacu for surface chemical analysis via XPS. Similar experimental conditions of the porous molybdenum samples were replicated on lithated graphite to compare results. An outline of experimental method on ATJ graphite can be found elsewhere [14]. Lithiated graphite is an important plasma–material interface, since in the context of NSTX graphite is dominant plasma-wetted surface material. Another goal of this paper is to indicate any differences in deuterium interaction with lithium-based surfaces between two different substrates (e.g. graphite vs porous molybdenum) and the possible role of surface chemistry on this interaction.

3. Results and discussion

XPS of a virgin porous molybdenum sample, shown in Fig. 1, shows two distinct peaks at 231.5 ± 0.6 eV and 235 ± 0.6 eV corresponding to Mo 3d photoelectron lines. Deposition of 3 μm of lithium onto the heated sample results in the absence of the corresponding Mo-based peaks and the appearance of a Li 1s peak (Figs. 1 and 2). Experimental parameters for lithium deposition on a hot (250 °C) sample were chosen to replicate the lithium fill conditions of the LLD. Lithium's alkali metal properties dictate high reactivity with ambient oxygen, requiring the study of chemical shifts of lithium-treated surfaces through the O1s spectrum. This methodology has proven effective in earlier studies of the lithiated graphite system [1,2,14].

Fig. 3 consists of XPS O1s spectra of porous Mo substrate for various surface treatments. There are two primary treatments: (1) deposition of lithium simulating fill conditions of the LLD in NSTX and, (2) low-energy irradiation at comparable fluences of deuterium. In Fig. 3, curve "a" representing the "as-is" condition for the porous Mo substrate, a prominent peak positioned at 530 ± 0.6 eV is observed. This peak has a broad shoulder toward

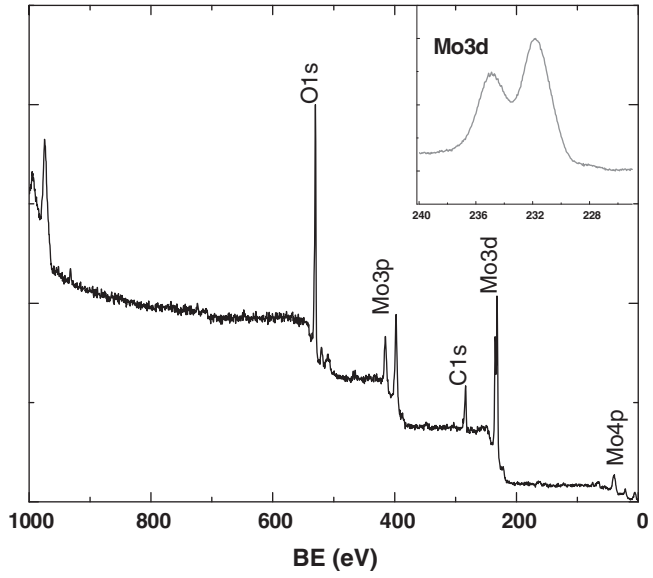

Fig. 1. XPS full spectrum of "as is" porous molybdenum sample. Associated photoelectron peak lines labeled. Insert shows Mo 3d region spectrum.

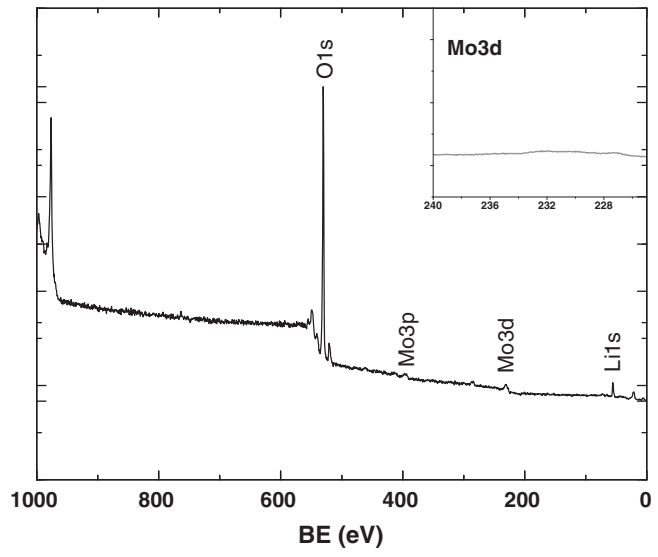

Fig. 2. XPS wide spectrum of porous molybdenum sample after 3-μm of lithium deposition at 250 °C. Associated photoelectron peak lines are labeled. Insert shows Mo 3d region spectrum at same scale as Fig. 1.

higher binding energies, an indication that a number of prominent oxide peaks exist for Mo surfaces [15]. We associate this broad peak to Mo–O interactions. Deposition of a 3-μm lithium film on the porous Mo surface at 250 °C results in a net shift of about 0.5 eV in the O1s spectrum. This binding energy is about 530.5 ± 0.6 eV and indicative of a lithium–oxygen interaction.

Following deuterium irradiation up to a fluence of 1.5×10^{16} D_2^+/cm^2 at 200 °C, a new peak is observed in the O1s spectrum and correlated only to D irradiation (i.e. no other irradiation conditions yielded this peak) in the presence of lithium. The new peak at 532.2 ± 0.6 eV is attributed to a functionality between Li–O–D. This functionality has been observed when depositing lithium coatings on ATJ graphite substrates in NSTX and under controlled conditions [14,15]. A shift for the Li–O peak of about 1.0 eV to a value of 529.5 eV has been also observed when irradiating lithium-based coatings with deuterium ions. The functionality at 532.2 eV is attributed to a chemically-sensitive binding channel for deuterium. The nature of the bond is a result of the high polarizability of lithium when interacting with other materials. For example in lithiated graphite, lithium will preferentially bind with C and O atoms and deuterium with C and O in the vicinity of lithium via dipole interactions. This result has been confirmed with quantum MD simulations and calculations using the electronegativity equalization method (EEM) by Yang and Krstic [16]. Therefore, we conjecture that the new peak observed in Fig. 3 curve "c" consists of a similar functionality (e.g. Li–O–D interactions) compared with lithiated graphite given the electronegativity of Mo is 2.16, similar to C at 2.55. However, the functionality is likely not as strong for the Li–C interaction (given the dissimilar electronegativity between Li and C) and thus we expect this effect to be weaker for Mo. This is evident in the next figure.

Fig. 4 illustrates the effect of deuterium irradiation on the lithiated porous Mo sample surface corresponding to low ($\sim 3.6 \times 10^{15}$ cm^{-2} "curve b") and high D irradiation fluence ($\sim 1.0 \times 10^{17}$ cm^{-2} "curve c") when depositing lithium at a high temperature (~250 °C) followed by D irradiation at 200 °C. The data is compared to a lithiated graphite sample exposed to high D irradiation fluence ($\sim 1.0 \times 10^{17}$ cm^{-2}). In the lithiated graphite case, the Li–O–D peak is located at higher binding energy and this peak is dominant over the metallic oxide peak. The 532.2 ± 0.6 eV peak for the case of Li–O–D interactions on the Mo substrate is consistent with the interpretation that the Li–O–D functionality is a "weaker" effect when depositing Li on a porous Mo substrate compared to the ATJ graphite substrate. This can be interpreted as the Li–O–D channel for D binding saturating promptly and likely D atoms retained by other binding states such as the conventional ionic bonds of Li–D or implanted D in solution within the Li coating.

Figs. 5 and 6 present the comparison for various recipes of lithium deposition on the porous Mo substrate. Due to the lower surface tension of lithium various wetting recipes were studied. These recipes needed to be compatible with heating limitations of the LLD on NSTX, therefore only a narrow temperature range was explored. Although the melting point of lithium is 180 °C, the wetting temperature on transition metals can be much higher for alkali metals [9]. Fig. 5 shows the Mo 3p peaks for three cases: "curve a" 2-μm of lithium deposition and 1.5×10^{16} D_2^+/cm^2 irradiation at room temperature; "curve b" 2-μm of lithium deposition at room temperature and 1.5×10^{16} D_2^+/cm^2 irradiation at 250 °C, and "curve c" 3-μm of lithium deposition at 250 °C and 1.5×10^{16} D_2^+/cm^2 irradiation at 200 °C. The room temperature result of "curve a" in Fig. 5 indicates (by the absence of the Mo 3p peak) that lithium deposition leads to a conformal lithium coating on the porous Mo substrate at least through the probe depth for XPS ranging from 5 to 10 nm for our case. If a similar deposition is conducted and then followed by heating to about 250 °C with deuterium irradiation (simulating conditions on the LLD in NSTX) the XPS data suggests that lithium is either percolating effectively through the porous Mo matrix away from the XPS probing region and/or D-induced erosion is effectively sputtering away any available lithium from that surface. This leads to a "mixed" layer of Mo and Li atoms at least in the probe depth of XPS since we also observed a Li 1s peak for this case. The sputter yield from deuterated liquid Li surfaces at 250 °C is about 0.2 Li atoms/ion at 500 eV/amu [17]. For a fluence of about 1.5×10^{16} D_2^+/cm^2, the total eroded thickness is only about 0.2-nm. Therefore removal of lithium by

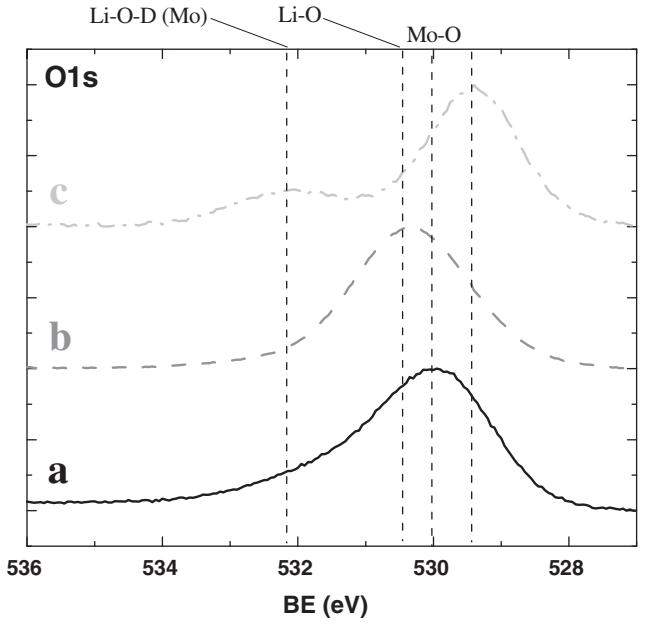

Fig. 3. XPS O1s spectrum of porous molybdenum for various sample conditions, (a) as received porous molybdenum sample, (b) after 3 μm of lithium deposition at 250 °C, (c) after Li deposition up to a 1.5×10^{16} D_2^+/cm^2 fluence at 200 °C.

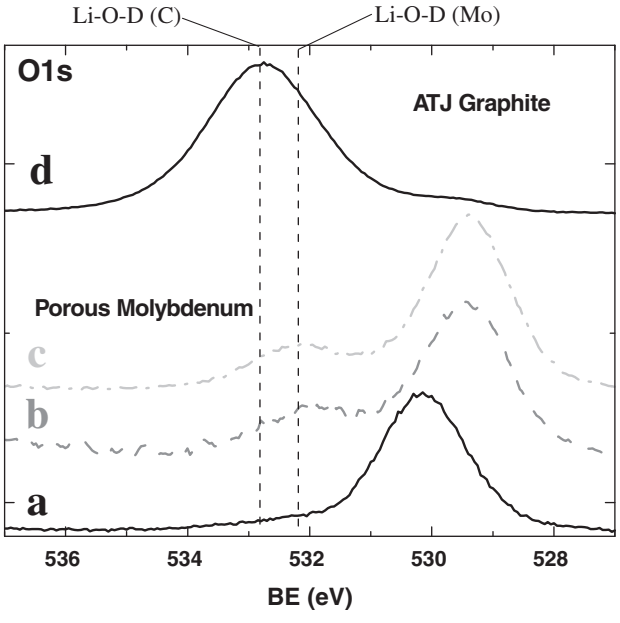

Fig. 4. O1s spectrum for porous molybdenum sample conditions compared to ATJ graphite. (a) Porous molybdenum sample after 3-μm of lithium deposition, (b) 3.6×10^{15} D_2^+/cm^2 at 250 °C, (c) 1×10^{17} D_2^+/cm^2 at 250 °C and (d) ATJ graphite post 2-μm of lithium deposition and 1×10^{17} D_2^+/cm^2 at room temperature.

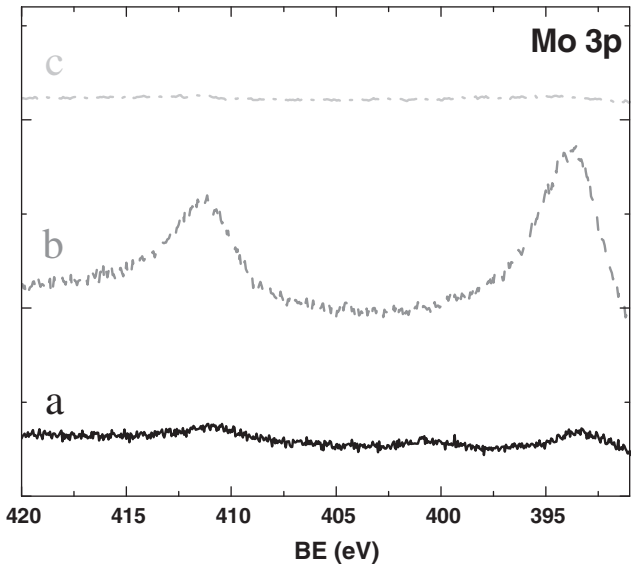

Fig. 5. Mo 3p spectrum for three recipes of lithium deposition and deuterium irradiation on porous molybdenum sample surface, (a) 3-μm of lithium deposition and 1.5×10^{16} D_2^+/cm^2 at room temperature, (b) 2-μm of lithium deposition at room temperature and 1.5×10^{16} D_2^+/cm^2 at 250 °C, and (c) 3-μm of lithium deposition at 250 °C and 1.5×10^{16} D_2^+/cm^2 at 250 °C.

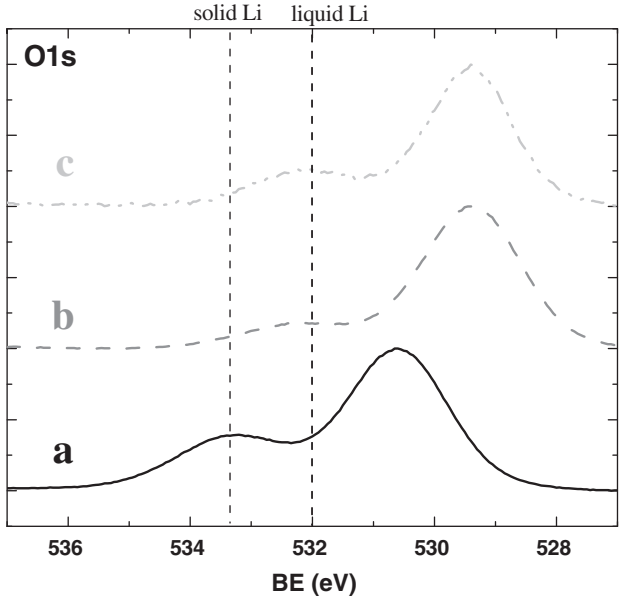

Fig. 6. O1s spectrum for three recipes of lithium deposition and deuterium irradiation on porous molybdenum sample surface, (a) 3-μm of lithium deposition and 1.5×10^{16} D_2^+/cm^2 at room temperature, (b) 2-μm of lithium deposition at room temperature and 1.5×10^{16} D_2^+/cm^2 at 250 °C, and (c) 3-μm of lithium deposition at 250 °C and 1.5×10^{16} D_2^+/cm^2 at 250 °C.

sputtering is unlikely. However, there is the probability that the reflected energy from incident D particles interacting with the high-Z Mo substrate could lead to enhanced erosion of the relatively thin liquid Li surface layer. This particular effect will be investigated with *in situ* tools in our laboratory in a future set of experiments. The last case suggests that if lithium is deposited "hot", at 250 °C, lithium will effectively "wet" the porous Mo substrate as evidenced by the absence of the Mo 3p peak shown in Fig. 5.

Fig. 6 compares the observed Li–O–D functionality for the three cases discussed above. Interestingly the results are not the same when comparing lithium in the solid and liquid states on the porous Mo substrate. The XPS O1s spectra shown in Fig. 6 indicate a new peak found after D irradiation at about 533.2 eV compared to 532.2 eV for lithium as a liquid coating. The metallic oxide peak is also shifted to higher binding energy. The origin of these shifts is still being investigated. We conjecture that likely the dominant oxide layer on the solid lithium surface could be playing an important role in binding D atoms via the Li–O–D channel discussed above. The results for liquid lithium are similar although curve "b" consists of the "non-wetting" case. The reader is reminded however that the non-wetting case still results with a *mixed* Mo and Li layer at the surface. Therefore one expects to still find the Li–O–D functionality for the non-wetting deposition case.

4. Conclusion

Lithium's unique deuterium uptake capabilities make it an ideal plasma-facing interface for applications with low-recycling hydrogen regimes in tokamak fusion devices. XPS analysis of deuterium irradiated lithiated graphite and porous molybdenum reveal similar Li–O–D chemical functionality in the O1s XPS spectrum. This behavior varies depending on the lithium treatment recipe used on porous Mo substrates under conditions that simulate those of the LLD in NSTX. This paper finds that the Li–O–D channel for D binding saturates promptly and likely D atoms are retained by other binding states such as Li–D ionic bonds or D in solution within the lithium coating. The XPS results also show that the effect of lithium's electropositive nature on D binding is rather weak when compared to lithiated graphite. The other important result from this work is that deposition of lithium hot at a temperature near 250 °C on the porous Mo substrate leads to effective wetting. The case for cold lithium deposition followed by heating and D irradiation yields a mixed non-uniform layer of Mo and Li atoms. Depositing lithium cold simply results in a solid conformal layer with marginal D retention capability. Further studies will explore how the Li–O–D functionality changes with phase for lithium coatings on porous Mo substrates. In addition, more work is needed to assess if any additional binding channels exist for deuterium in the form of the ionic Li–D bond or solution retention of D in the liquid Li matrix. The complex surface morphology of the porous Mo substrate also will be studied in the context of lithium coatings and pumping of hydrogen.

Acknowledgements

The authors thank Birck Nanotechnology for facilities and staff, Sami Ortloeva for data acquisition. Work supported by US DOE Contracts DE-FG02-08ER54990, DE-AC02-09CH11466.

References

[1] J.P. Allain et al., J. Nucl. Mater. 390–391 (2009) 942–946.
[2] C.N. Taylor et al., J. Nucl. Mater. (2010), doi:10.1016/j.jnucmat.2010.09.049.
[3] H.W. Kugel et al., J. Nucl. Mater. 390–391 (2009) 1000–1004.
[4] H.W. Kugel et al., Phys. Plasmas 15 (2008) 056118.
[5] J.P. Allain et al., J. Nucl. Mater. 290–293 (2001) 180–184.
[6] D.G. Whyte et al., Fusion Eng. Des. 72 (2004) 133–147.
[7] J.P. Allain, M.D. Covenry, D.N. Ruzic, Phys. Rev. B 76 (2007) 205434.
[8] M.J. Baldwin, R.P. Doerner, S.C. Luckhardt, R.W. Conn, Nucl. Fusion 42 (2002) 1318.
[9] R. Majeski et al., Nucl. Fusion 45 (2005) 519–523, doi:10.1088/0029-5515/45/6/014.
[10] S. Mirnov, J. Nucl. Mater. 390–391 (2009) 876–885.
[11] H.W. Kugel et al., Fusion Eng. Des. (2010), doi:10.1016/j.fusengdes.2010.04.004.
[12] M.A. Jaworski et al., J. Nucl. Mater. 378 (2008) 105–109.
[13] S.S. Harilal et al., Applied Surface Science 255 (2009) 8539–8543.
[14] C.N. Taylor, J.P. Allain, J. Appl. Phys., accepted for publication.
[15] J.-G. Choi, L.T. Thompson, Appl. Surf. Sci. 93 (1996) 143–149.
[16] P. Krstic, Z. Yang, et al. Phys. Rev. Lett., in preparation.
[17] J.P. Allain, M.D. Coventry, D.N. Ruzic, Phys. Rev. B 76 (2007) 205434.